Technical University of Denmark

DTU

Soot Reactivity in Conventional Combustion and Oxy-fuel Combustion Environments

Abian, Maria; Jensen, Anker Degn; Glarborg, Peter; Alzueta, Maria U.

DTU Library
Technical Information Center of Denmark

Soot Reactivity in Conventional Combustion and Oxy-fuel Combustion Environments

María Abián,[†,‡] Anker D. Jensen,[†] Peter Glarborg,[†] and María U. Alzueta*,[‡]

[†]Department of Chemical and Biochemical Engineering, Technical University of Denmark, Building 229, DK-2800 Lyngby, Denmark
[‡]Aragon Institute of Engineering Research, University of Zaragoza, Río Ebro Campus, C/Mariano Esquillor s/n, 50018 Zaragoza, Spain

ABSTRACT: A study of the reactivity of soot produced from ethylene pyrolysis at different temperatures and CO_2 atmospheres toward O_2 and CO_2 has been carried out using a thermogravimetric analyzer. The purpose was to quantify how soot reactivity is affected by the gas environment and temperature history of the carbon, as well as to compare the soot reactivity toward O_2 and CO_2. Soot samples were either oxidized in 5% O_2 or gasified in 10, 50, and 90% CO_2 atmospheres, during non-isothermal runs at 10 K/min. Soot oxidation was observed at temperatures of 400−500 K lower than soot gasification, showing higher reactivity toward oxygen than CO_2. Independent of the environment history of the soot samples, the soot samples formed at lower temperatures have higher reactivity toward both O_2 and CO_2 than the soot samples obtained at higher temperatures. The presence of CO_2 during the formation of the soot only affected the soot reactivity at the highest formation temperature (1475 K) and CO_2 concentration (78.5%). Under these conditions, the soot reactivity was observed to increase by a factor of about 2.6 compared to soot formed in N_2 at the same temperature. We attribute the increased reactivity to a higher micropore surface area, facilitated by the gasification reaction at a high temperature. The intrinsic kinetics for oxidation and gasification of soot were obtained by applying the volumetric reaction model.

INTRODUCTION

It is well-known that soot is one of the main pollutants generated in most combustion processes. Studies related to soot are always a challenge, because it is a very complex material that can be formed through various reaction pathways and under a variety of conditions and can present very different structures, among other factors. Within the combustion chamber, soot may undergo different fates; it may become oxidized by the reaction with O_2, CO_2, and other oxidizing compounds[1−3] or be emitted as sub-micrometer particles.

Most studies of soot have been related to conventional combustion atmospheres (i.e., O_2 and N_2). Recently, oxy-fuel combustion has appeared as a promising technology to mitigate the climate change because of the generation of a CO_2-rich gas stream suitable for sequestration, with a feasible application in both existing and new plants.[4,5] For this reason, investigations related to soot formation and destruction in typical oxy-fuel CO_2 atmospheres to identify the possible chemical effect of high CO_2 levels on soot behavior at combustion temperatures are important. It has been shown that gasification of some carbon materials results in fine structural rearrangements in the carbon, leading to the loss of surface area and volume in fine pores,[6,7] and thus, the trends in soot properties can vary significantly depending upon whether the soot is formed in atmospheres with different CO_2 concentrations or in N_2. Borrego and Álvarez[8] investigated the properties of char when formed in a drop tube reactor at 1573 K from coal combustion in O_2/N_2 or from oxy-combustion in O_2/CO_2. Using a thermogravimetric analyzer (TGA) and micropore surface area measured by CO_2 adsorption, they observed that the chars were similar in terms of reactivity by combustion with air at 823 K. However, the chars had different surface areas as determined by

N_2 adsorption, and the size distribution of pores was shifted to a larger size for the char obtained in O_2/CO_2.

In oxy-fuel (O_2/CO_2) conditions, CO_2 as a reactant may influence soot conversion once formed. Most studies found in the literature on carbon reactivity toward CO_2 are related to coal char reactivity.[9−12] All of them observed a CO_2 gasification effect on the coal/char conversion when replacing N_2 by CO_2. However, studies on soot gasification with CO_2 are limited.

In this work, we have carried out an experimental study on the reactivity of soot in different gas environments, which allows us to identify quantitatively how soot reactivity is affected by the environment and temperature history of the carbon, as well as to compare the soot reactivity toward O_2 and CO_2.

EXPERIMENTAL SECTION

The reactivity of soot samples obtained from different reaction environments toward O_2 and CO_2 was measured using a Netzsch STA 449 F1 TGA. The soot samples were prepared in a quartz flow reactor from the pyrolysis of 30 000 ppm of ethylene at 1275, 1375, and 1475 K, in different CO_2 concentration environments (specifically 0, 25, 50, and 78.5% CO_2; Table 1), following the methodology described by Ruiz et al.[13] and Esarte et al.[14] The total flow rate in these experiments was 1000 mL/min [standard temperature and pressure (STP)], resulting in a gas residence time dependent upon the reaction temperature as t_r (s) = 4550/T (K). The soot produced in each experiment was collected in a quartz fiber thimble (mesh light lower than 1 μm) placed at the outlet of the reactor. The experiments were

Table 1. Formation Conditions of the Soot Samples Investigated

soot sample	ethylene (ppm)	CO$_2$ (%)	temperature (K)
sample 1			1275
sample 2		0	1375
sample 3			1475
sample 4			1275
sample 5		25	1375
sample 6	30000		1475
sample 7			1275
sample 8		50	1375
sample 9			1475
sample 10			1275
sample 11		78.5	1375
sample 12			1475

run for the necessary time to collect a significant amount of soot (higher than 1 g).

The evaluation of the soot reactivity has been based on the measurement of the change in sample mass as a function of the temperature and time at a constant heating rate of 10 K/min up to 1275 K in 5% O$_2$ and up to 1675 K in 10, 50, and 90% CO$_2$, with nitrogen as balance. Alumina crucibles filled with the soot samples, as well as blank reference crucibles, were placed in a highly sensitive balance located in the chamber of the apparatus. The mass of the sample and the crucible temperature were recorded continuously as reaction progressed. For each set of experiments, a calibration curve was made to avoid any possible fluctuations caused by the TGA that could influence the experimental measurements.

The initial sample mass and heating rate used in the TGA experiments was chosen to minimize possible mass-transfer limitations in the oxidation step of the experiments that occur by oxygen gas concentration gradients through the crucible down to the particle bed, through the particle bed, and inside the soot particles.[15] A high initial sample mass and high heating rate may lead to a reaction dominated by diffusion limitations, because the deeper layers of sample would be inaccessible for the oxidant. This may be partly solved by reducing the sample mass, but this may, on the other hand, affect the repeatability of the results.[16]

To evaluate the influence of mass-transfer limitations on the combustion experiments, different sample masses of 1, 2, 3.5, 4, and 6 mg (Figure 1) were tested for soot sample 12 in Table 1. When plotting curves of the time derivative of the mass loss of a carbon as a function of the temperature at a constant heating rate, the peak
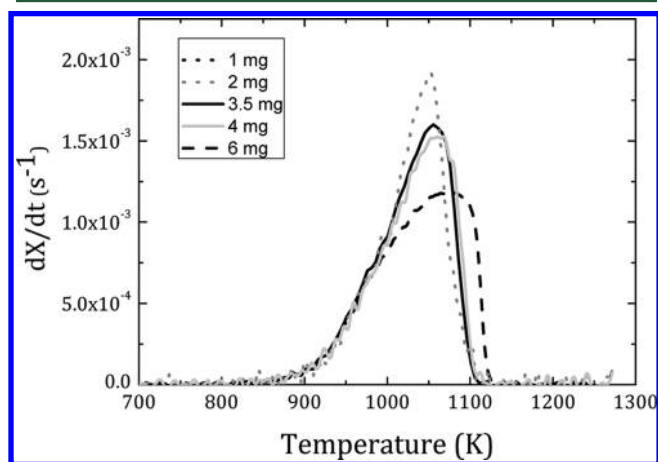
Figure 1. Influence of the soot sample mass for TGA experiments. Oxidation of soot sample 12 (Table 1) with 5% O$_2$ up to 1275 K at 10 K/min. Mass loss rate curves from initial soot sample masses of 1 and 2 mg exactly overlap.

temperature, PT, where the burning rate is maximum, is a way to express the reactivity of a fuel.[17] Higher peak temperatures indicate lower reactivity. In such a way, figures in this paper present the soot reactivity as the rate of mass loss, dX/dt (s^{-1}), defined by

$$\frac{dX}{dt} = \frac{1}{m_o}\frac{dm}{dt} \qquad (1)$$

Here, m_0 is the initial mass of soot, and m is the mass of soot at time t. The experimental mass and the mass loss rate curves were smoothed for clarity.

It can be inferred from the results in Figure 1 that the rate of mass loss and peak temperature are quite similar for masses lower than 4 mg and, in particular for initial sample masses of 1 and 2 mg, the general profile shape and peak temperature exactly match each other, demonstrating the good repeatability of the soot oxidation in the TGA and the absence of mass-transfer limitations. For higher initial soot masses, i.e., 6 mg, the results indicate the presence of diffusion limitations because the mass loss rate decreases and the PT increases in comparison to the results attained with lower masses.

On the basis of these results, usually less than 3.5 mg of soot samples was applied in the oxidation/gasification experiments.

■ RESULTS AND DISCUSSION

To establish how the reactivity toward O$_2$ is affected by both the soot formation environment and temperature history of the soot, the soot particles were oxidized in 5% O$_2$ at a heating rate of 10 K min^{-1} to a maximum temperature of 1275 K. The influence of the temperature history of the soot is considered initially. Figure 2 shows the mass loss rate dX/dt versus T as a function of the soot formation temperature for the soot formed in the 0, 25, 50, and 78.5% CO$_2$ atmosphere. In general, the peak temperature is shifted to higher values as the soot formation temperature is increased. For example, in Figure 2a, the soot formed in a N$_2$ atmosphere at 1275 K (set 1 in Table 1) has the PT at 927 K, whereas the soot formed in a N$_2$ atmosphere at 1475 K (set 3 in Table 1) has the PT at 1102 K. This behavior is independent of the CO$_2$ concentration in the reaction environment, and thus, a decrease in soot sample reactivity with an increasing soot formation temperature is observed.

It can be seen that some of the soot samples present a double peak in the dX/dt versus T curve (DGT peak), particularly samples 8 and 11 in Table 1. Double DGT peaks have also been detected in studies of char reactivity. Russell et al.[18] concluded that single narrow peaks can be interpreted to represent homogeneous char, single broadened peaks would represent a more heterogeneous mixture and double peaks would correspond to a clear bimodal combination of two constituents with different reactivity, as was also suggested by Zolin et al.[15] and Zhang et al.[19]

The presence of two peaks in the dX/dt versus T curve can indicate the transformation of a reactive phase into a less reactive phase with an increasing soot formation temperature. For 1475 K, the formation of two peaks is less evident; mostly, a single peak is observed and positioned at higher temperatures, indicating that most of the soot is converted into the less reactive phase. This loss in soot reactivity when increasing its formation temperature has also been observed in other studies on soot and char reactivity.[7,15,20] Thermal annealing has been suggested as one of the main mechanisms involved in char reactivity loss (deactivation) during combustion. It has been reported that the exposure of the fuel to high temperatures in the boiler causes a thermal annealing of the particles, characterized by the loss of surface area, loss of active sites,
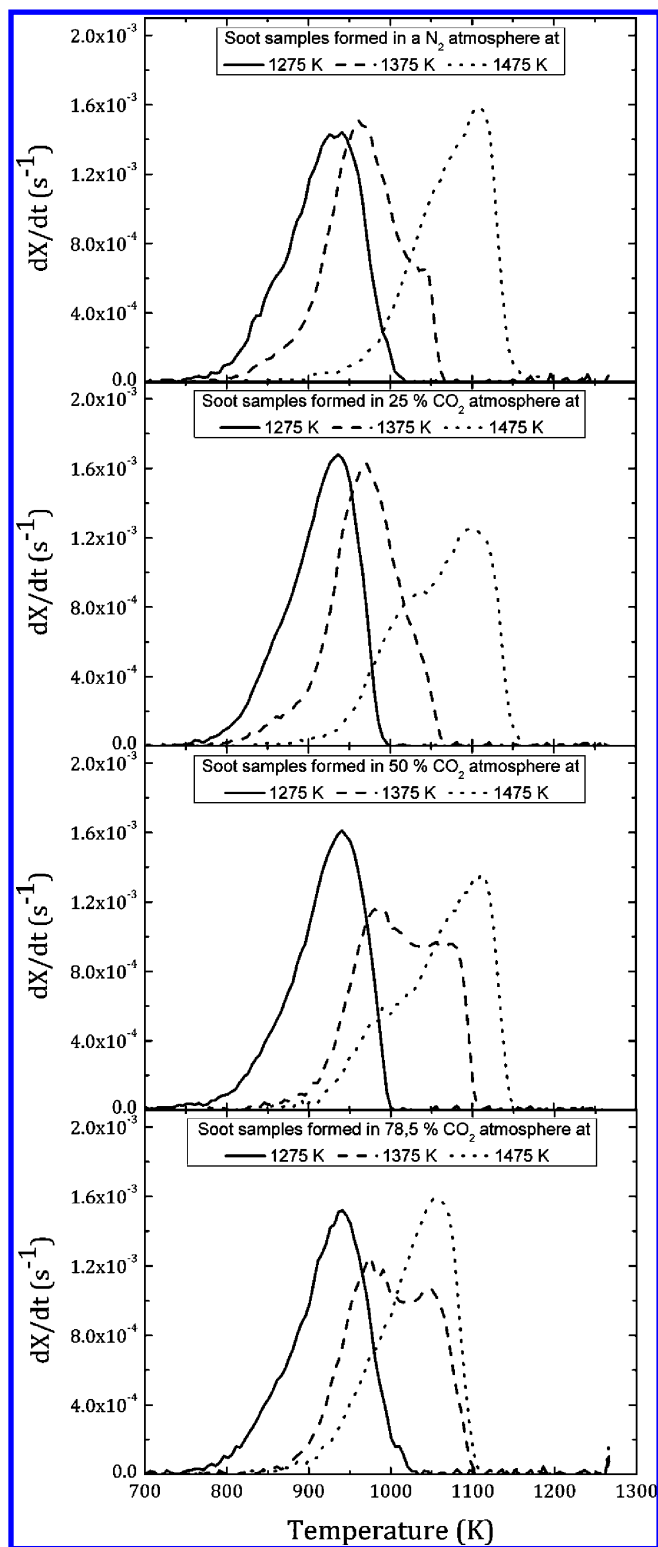
Figure 2. Oxidation profiles of the soot samples prepared in different CO_2 environments as a function of the reaction temperature: (a) 0% CO_2 (sets 1−3 in Table 1), (b) 25% CO_2 (sets 4−6 in Table 1), (c) 50% CO_2 (sets 7−9 in Table 1), and (d) 78.5% CO_2 (sets 10−12 in Table 1). Soot particles were oxidized with 5% O_2 up to 1275 K at 10 K/min.

and/or loss of active site reactivity.[15] Zolin et al.[15] performed an extensive experimental study of char thermal deactivation based on reactivity experiments of different fuel chars. They

observed a clear tendency to develop two phases as the heat treatment temperature (HTT) increased, with the less reactive phase of those coals gradually approaching the reactivity of commercial graphite, hence suggesting a high degree of crystalline order. They explained the gradual formation of two phases in the TGA found for some of the coal chars as follows: At low HTTs, where only one peak was attained, the basic structural units or crystallites, responsible for the graphitization or annealing of the char, are of small size and probably also their chemical composition still resembles the other parts of the char and, thus, does not lead to a clear-cut separate ordered region in the char. At higher HTTs, further volatile release may be accompanied by the removal of the organic units attached to the crystallites and the rest of the char, allowing for the crystallites to increase in size and concentration and to reorganize into more graphite-like alignments. At this point, clear-cut regions of crystalline order may exist, and as a result, the char splits into two fractions with different reactivity.

These findings would be expected to be valid also for soot. Ruiz et al.[7] have reported that, at elevated soot formation temperatures, a graphitization process occurs that may lead to a less reactive soot. It has also been reported in the literature that the hydrogen content can be directly related to the availability of active sites of the solid and, thus, to its reactivity.[21,22] In this context, Ruiz et al.[7] carried out reactivity experiments of the soot formed from acetylene pyrolysis at different temperatures. They noticed through elemental analysis that, in general, higher soot formation temperatures result in higher carbon contents and lower hydrogen contents and related this tendency to the reactivity results because the soot samples formed at lower temperatures were the most reactive. Elemental analyses of representative soot samples (samples 2 and 3 in Table 1) indicate that higher soot formation temperatures result in higher carbon contents and lower hydrogen contents, in agreement with the conclusions cited above. Table 2 shows the results of the elemental analyses of these soot samples, as well as the C/H ratio on a molar basis.

Table 2. Elemental Analysis and C/H Ratio (Molar Basis) of Soot Samples Obtained at Different Temperatures in a N_2 Atmosphere

soot samples	elemental analysis (wt %) (dry basis)				C/H (molar basis)
	C	H	N	S	
sample 2	97.77	1.01	0	0	96.80
sample 3	99.71	0.37	0	0	269.49

The influence of the CO_2 concentration during soot formation is illustrated in Figure 3, which shows the mass loss rate in dX/dt versus T as function of the soot formation environment for specific soot formation temperatures. In this case, no clear tendencies can be observed because, dependent upon the soot formation temperature, the CO_2 atmosphere present in the formation of the soot samples plays a different role. At 1275 K, the soot formation environment does not significantly affect the soot sample reactivity, and the peak temperatures for the different CO_2 soot formation atmospheres are approximately at 935 K. At 1375 K, although in general there are no clear differences in reactivity of the soot formed in the different CO_2 atmospheres, for the soot samples formed with 50 and 78.5% CO_2, a second less reactive phase in the soot oxidation begins to appear, indicated by the two peaks in the
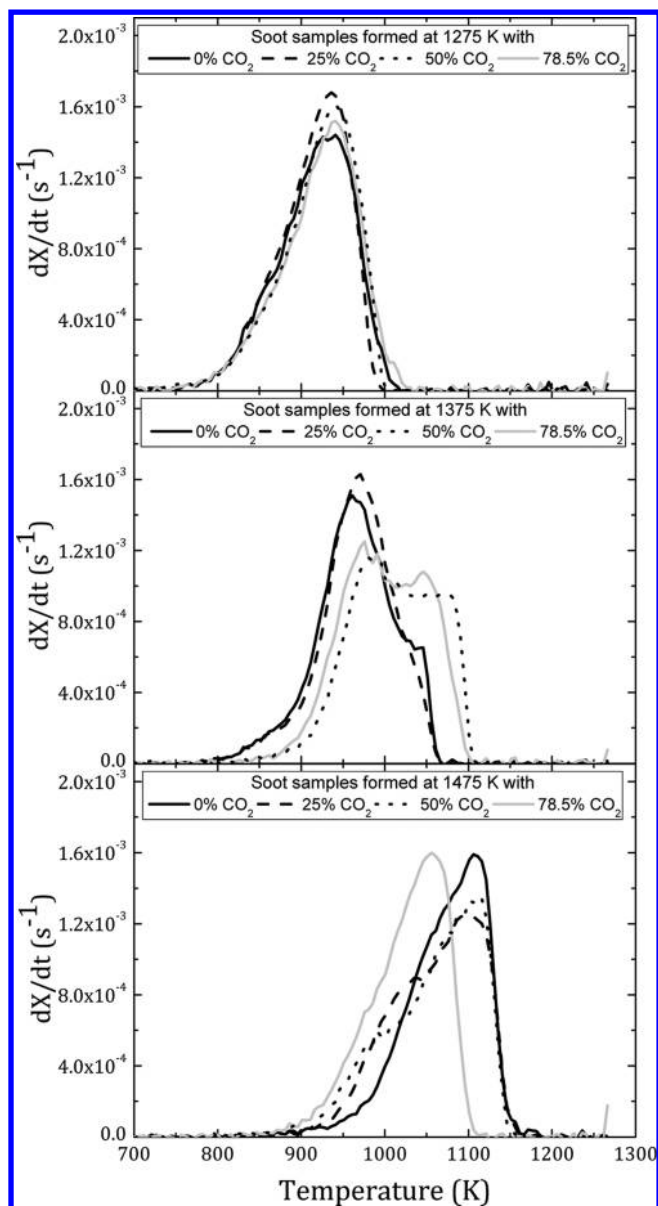
Figure 3. Oxidation profiles of the soot samples prepared at different temperatures as function of the CO_2 reaction environment: (a) 1275 K (sets 1, 4, 7, and 10 in Table 1), (b) 1375 K (sets 2, 5, 8, and 11 in Table 1), and (c) 1475 K (sets 3, 6, 9, and 12 in Table 1). Soot particles were oxidized with 5% O_2 up to 1275 K at 10 K/min.

dX/dt versus T curve. At 1475 K, an appreciable mass loss of the soot samples formed with 25, 50, and 78.5% CO_2 takes places at lower temperatures than the initiation mass loss temperature for the soot formed in the N_2 atmosphere. The promoting effect of CO_2 increases with the CO_2 concentration in the soot formation environment, and the soot sample reactivity, represented by the lower PT is highest for the 78.5% CO_2 concentration (78.5%).

The increase in reactivity could imply an effect of CO_2 at high temperatures during the formation of the soot sample 12 (Table 1). This is probably due to the generation of micropores with a high surface area because of gasification by CO_2. Adsorption isotherms of the soot samples formed at 1475 K with N_2 (soot 3 in Table 1) and with 78.5% CO_2 (soot 12 in Table 1) have been determined by both CO_2 adsorption at 273 K and quantified using the Dubinin−Radushkevich method and

by nitrogen adsorption at 77 K in combination with the Brunauer−Emmett−Teller (BET) adsorption isotherm model.

The CO_2 surface area measurements confirm that the soot sample formed in the 78.5% CO_2 atmosphere has a higher micropore surface area (117 m^2/g for soot sample 12; Table 1) than the soot sample formed in the N_2 atmosphere (20 m^2/g for soot sample 3; Table 1). In the case of surface areas determined from N_2 adsorption isotherms, the soot sample formed in the 78.5% CO_2 atmosphere (sample 12 in Table 1) presents a BET surface area of 9.6 m^2/g, while the BET surface area for the soot sample formed in the N_2 atmosphere (sample 3 in Table 1) is 14.4 m^2/g. These area values are very low, and the differences between samples are not considerable.

It has been suggested in the literature that the graphitization process is accelerated by the presence of O_2 or CO_2 in the gas phase, because oxidizing gases preferentially attack less ordered carbon, removing cross-linkages between graphitic crystallites and accelerating crystallite grow.[6] In addition, the graphitization process can lead to lower surface area values.[7] Under the conditions of 78.5% CO_2 and 1475 K, it appears that, even if the presence of CO_2 may lead to some additional graphitization, the positive effect of CO_2 from generating microporosity is dominating, leading to enhanced reactivity.

To assess the influence of CO_2 gasification on soot conversion, soot particles were gasified in 10, 50, and 90% CO_2 at a heating rate of 10 K min^{-1} to a maximum temperature of 1675 K, using sample 12 in Table 1. On the basis of experience from the oxidation experiments, sample masses of around 2−3 mg were used. Figure 4 shows the results of these
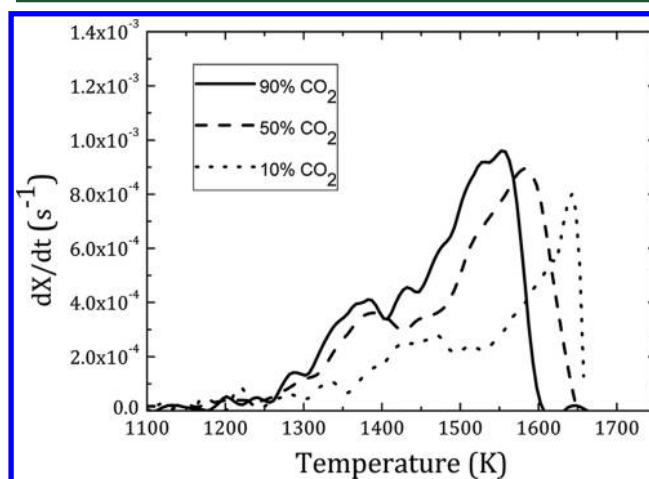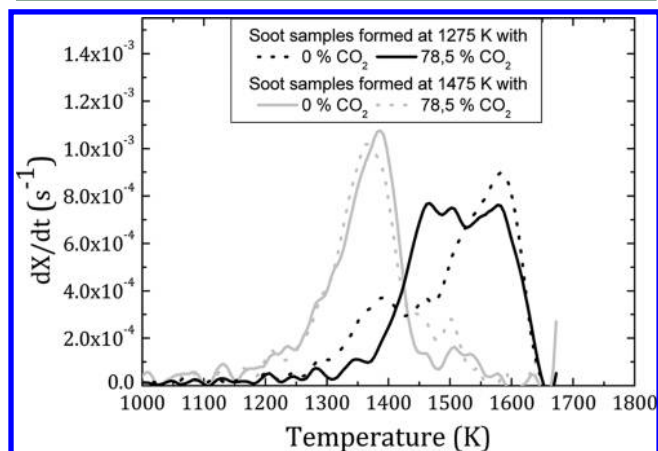

Figure 4. Gasification profiles of soot sample 12 (Table 1) in atmospheres consisting of 10, 50, and 90% CO_2 up to 1675 K at 10 K/ min.

experiments. It can be observed that, independent of the CO_2 concentration, gasification is appreciable at temperatures above 1250 K. In general, this initiation temperature is slightly higher than the one found for coal char gasification in TGA, i.e., around 1030 K[12] or 1073 K.[9,11] It is also observed, as expected, that the gasification rate increases with the CO_2 concentration. The lowest peak temperature of 1525 K is obtained with 90% CO_2, whereas for the lowest CO_2 concentration (10%), the soot sample is not totally consumed even at the highest temperatures analyzed.

To evaluate the influence of the environment/temperature history of the soot in relation to its reactivity toward CO_2, TGA

gasification experiments have been performed at a heating rate of 10 K min^{-1} up to 1675 K in 50% CO_2 with soot samples obtained at 1275 K in 0% CO_2 (sample 1) and 78.5% CO_2 (sample 10) and soot samples obtained at 1475 K in 0% CO_2 (sample 3) and 78.5% CO_2 (sample 12). The dX/dt versus T results for these experiments are presented in Figure 5. It can

Figure 5. Gasification profiles of selected soot samples prepared at different temperatures and CO_2 reaction environments (sets 1, 3, 10, and 12 in Table 1). Soot particles were gasified with 50% CO_2 up to 1675 K at 10 K/min.

be observed that, independent of the soot formation environment, the soot produced at lower temperatures (1275 K) reacts at lower temperatures than that produced at higher temperatures (1475 K). These results are consistent with the observations drawn from Figure 2 for the oxidation experiments. For the soot samples formed at 1275 K, there is no appreciable influence of the reaction environment (0−78.5% CO_2), because this temperature is too low for CO_2 gasification to take place, and thus, no microporosity is expected. For the soot samples obtained at 1475 K, it can be observed in the dX/dt versus T profile that the soot sample formed in the N_2 atmosphere (soot 3 in Table 1) presents a single broadened peak, and the soot sample formed in the 78.5% CO_2 atmosphere (soot 12 in Table 1) presents two peaks, with the smaller peak at lower temperatures and the higher second peak at higher temperatures. Although in general the reactivity of these soot samples toward CO_2 is not considerably changed, the mass loss of the soot sample formed in the 78.5% CO_2 environment is appreciable at lower temperatures than for the soot sample formed in the N_2 atmosphere. It is also remarkable that the larger consumption of these soot samples is initiated at temperatures around their formation temperature (1475 K).

The oxidation and gasification kinetics of soot have been derived from the experimental mass loss data according to a volumetric reaction model (VRM)[23] given by

$$\text{rate} = \frac{-1}{m}\left(\frac{dm}{dt}\right) = \frac{1}{1-X}\left(\frac{dX}{dt}\right) = k_0 e^{-E_a/RT} \qquad (2)$$

$$X = \frac{m_0 - m}{m_0}$$

Here, rate (mg mg^{-1} s^{-1}) represents the reaction rate based on the instantaneous mass of soot. m_0 and m are the initial carbon mass (mg) and the carbon mass at a certain time, t, respectively. X is the carbon conversion at any time. R (kJ mol^{-1} K^{-1}) is the

ideal gas constant. E_a (kJ/mol) is the activation energy. k_0 (s^{-1}) is the pre-exponential factor. T (K) is the reaction temperature. When the oxidation/gasification data were fitted to the VRM model, k_0 and E_a were determined. In the kinetic analysis, we have neglected soot samples with two distinct phases of different reactivity. Samples with a minor second peak however were included, but in this case, the fitting only involved the conversion range of the main peak. Figures 6 and 7 show the
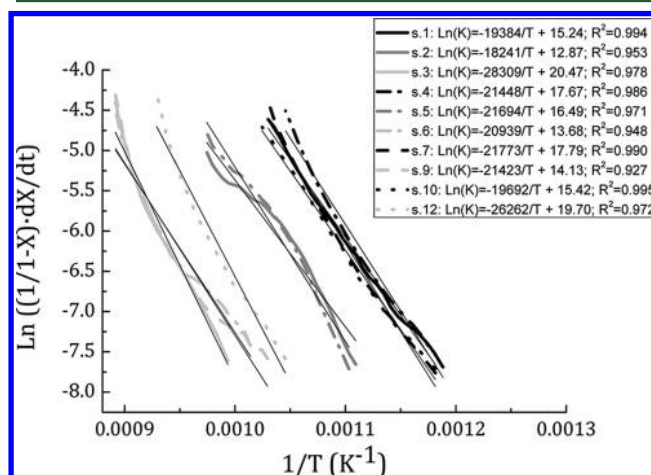
Figure 6. Arrhenius plots of oxidation rate constants with 5% O_2 for soot obtained under different temperature/CO_2 environment conditions (sets 1−12 in Table 1).
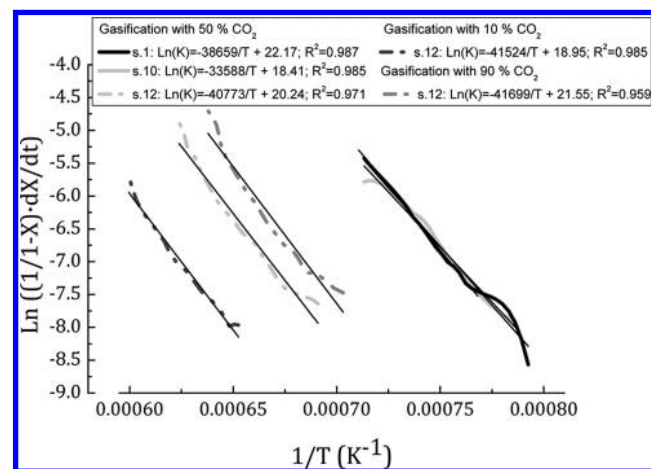
Figure 7. Arrhenius plots of gasification rate constants for soot obtained under different temperature/CO_2 environment conditions: sets 1, 10, and 12 in Table 1 for gasification with 50% CO_2 and set 12 in Table 1 for gasification with 10 and 90% CO_2.

Arrhenius plots for combustion and gasification, respectively, of soot samples obtained from the different temperature/environment conditions, along with the linear regression results for each soot.

Table 3 summarizes the activation energy for the oxidation of soot samples 1−12 and for the gasification of soot samples 1, 10, and 12. The oxidation of soot samples shows activation energies in the range of 152−235 kJ/mol, while the corresponding values for gasification are in the range of 279−347 kJ/mol, with most of the soot samples presenting E_a values in the 300−347 kJ/mol range.

In their review on soot oxidation, Stanmore et al.[1] found that activation energies for soot oxidation cover a range of 102−210

Table 3. Kinetic Constants of Soot Oxidation with 5% O_2 and Gasification with 50% CO_2[a]

|	E_a (kJ/mol)	common E_a (kJ/mol)	k_0 (s^{-1}) (VRM)
		Oxidation	
sample 1	161		7.61×10^7
sample 2	152		2.04×10^7
sample 3	235		1.76×10^6
sample 4	178		8.49×10^7
sample 5	180	182	1.99×10^7
sample 6	174		2.25×10^6
sample 7	181		6.77×10^7
sample 9	178		2.30×10^6
sample 10	164		6.50×10^7
sample 12	218		4.83×10^6
		Gasification	
sample 1	321		1.18×10^{10}
sample 10	279	326	1.05×10^{10}
sample 12	339		4.18×10^8

[a]Activation energies were based on VRM and pre-exponential factors assuming a common activation energy for the oxidation and gasification reactivities, respectively, in VRM.

kJ/mol, with values between 140 and 170 kJ/mol appearing frequently. Therefore, the range of activation energies for soot oxidation found in this study is in reasonable agreement with previous research work. To our knowledge, no values of activation energies have been reported in the literature for the soot gasification with CO_2.

To compare the relative reactivity of the different soot samples as a function of their temperature/environment history, the activation energy was fixed at a common value in eq 2 for the oxidation and gasification experiments, respectively, while the pre-exponential factor k_0 (s^{-1}) was obtained as a single parameter in the model. The input to the fitting procedure has been the values of time and soot conversion at a heating rate of 10 K min^{-1} and a mean activation energy E_a of 182 kJ/mol for the soot oxidation and E_a of 326 kJ/mol for the soot gasification. The best fit corresponded to the value of k_0 (s^{-1}) that minimized the sum of squares of the differences between experimental and calculated conversion values. As an example of the qualitative interpretation of the soot oxidation/gasification profiles, Figure 8 presents the data corresponding to the experimental and model predictions according to the VRM of soot samples 10 and 12 in Table 1 using a common activation energy for all soot samples of 182 kJ/mol when oxidized with 5% O_2 and 326 kJ/mol when gasified with 50% CO_2. It can be noticed that the model based on a common activation energy predicts fairly well the experimental results.

The calculated k_0 (s^{-1}) values are presented in Table 3 and summarized in Figure 9. It can be observed that the re-estimated k_0 values of both the oxidation and gasification experiments decrease as the soot formation temperature increases, independent of the CO_2 concentration in the soot formation environment, suggesting that thermal deactivation of the soot takes place as the soot formation temperature increases. However, there are no clear differences in relation to the gas environment of the soot samples.

The onset of reaction with O_2 for all soot samples studied is observed at temperatures about 450 K lower than the corresponding value for CO_2, confirming that oxidation is much faster than gasification at these temperatures. For example, in quantitative terms, oxidation of soot sample 10 in
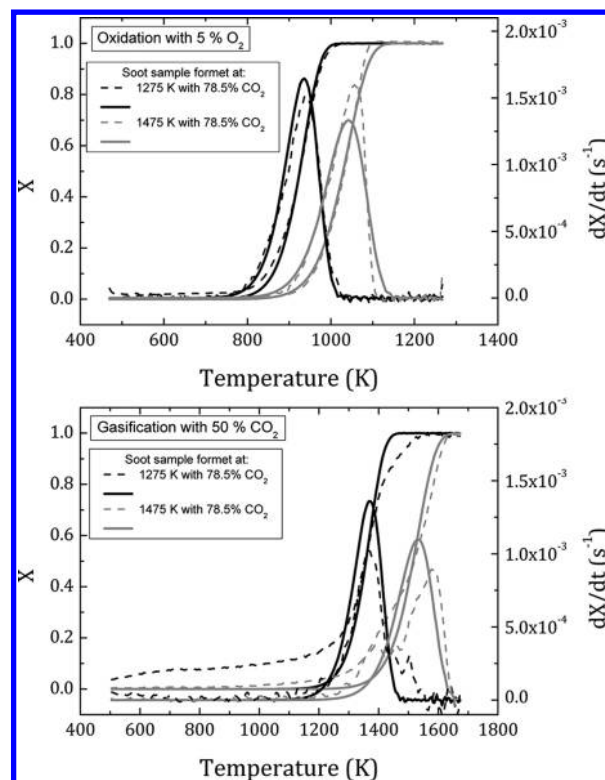
Figure 8. Oxidation (upper panel) and gasification (bottom panel) profiles of soot sample 10 in Table 1 (black lines) and soot sample 12 in Table 1 (gray lines). Experimental data are displayed as dashed thin lines. Model data (VRM) are displayed as continuous thick lines. Soot particles were oxidized with 5% O_2 up to 1275 K and gasified with 50% CO_2 up to 1675 K at 10 K/min.

Table 1 is about 5000 times faster than its CO_2 gasification at 1273 K.

The reaction order with respect to CO_2 has been derived from eq 3.

$$k_0 = A_0 P_{CO_2}^n \tag{3}$$

Here, k_0 is the re-estimated value obtained by fixing a common activation energy in eq 2 for the gasification of the soot sample obtained at 1475 K and 78.5% CO_2 (set 12 in Table 1), with 10, 50, and 90% CO_2 (values presented in Table 4). n is the order of the reaction expressed as an exponent of the reaction of CO_2 partial pressure P_{CO_2} (atm). Figure 10 shows the fitting of the experimental data to eq 3 for the experiments of soot 12 gasification with different CO_2 concentrations, along with the linear regression results. An order with respect to CO_2 of 0.98 is obtained. This order is similar to the reaction order of around 1 with respect to O_2 determined previously by several authors for the oxidation of soot[24,25] and higher than the apparent reaction order found in the literature for char gasification, which varies around 0.5.[26]

■ CONCLUSION

An experimental and kinetic study on the oxidation and gasification of soot samples from different temperature/environment formation conditions has been carried out. Soot samples were prepared from the pyrolysis of ethylene at 1275, 1375, and 1475 K and for CO_2 atmospheres of 0, 25, 50, and 78.5% CO_2.
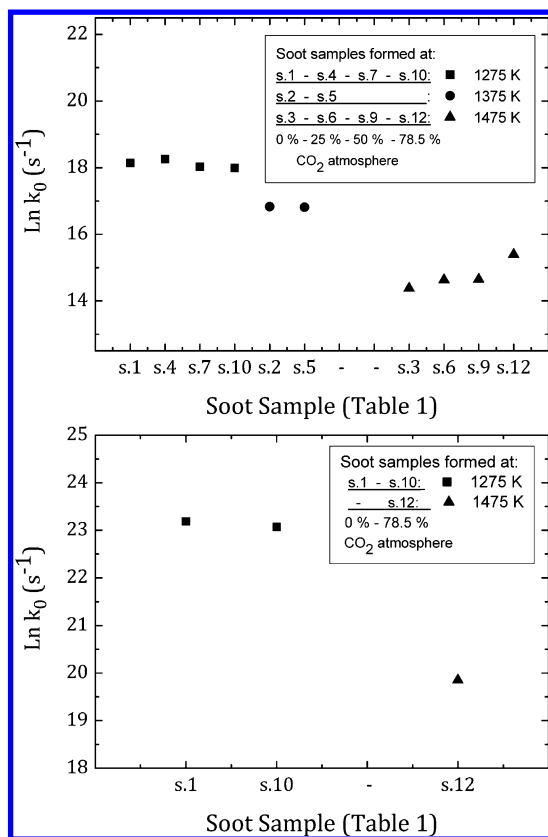
Figure 9. Estimated k_0 values for constant activation energy in VRM of both the oxidation (upper panel; E_a = 182 kJ/mol) and gasification (bottom panel; E_a = 326 kJ/mol) reactivities as a function of the temperature/environment history of the soot samples (Table 1).

Table 4. Kinetic Constants of Soot Gasification of Soot Sample 12 in Table 1 with 10, 50, and 90% CO_2[a]

[CO_2] (%)	E_a (kJ/mol)	common E_a (kJ/mol)	k_0 (s^{-1}) (VRM)
10	345		8.57×10^7
50	339	326	4.18×10^8
90	347		7.43×10^8

[a]Activation energies were based on VRM and pre-exponential factors assuming a common activation energy for gasification reactivities in VRM.

The reactivity of the soot samples was determined in non-isothermal experiments using a TGA. Oxidation was carried out in 5% O_2 at a heating rate of 10 K min^{-1} to a maximum temperature of 1275 K, and gasification was carried out in 10, 50, and 90% CO_2 at a heating rate of 10 K min^{-1} to a maximum temperature of 1675 K. The experiments showed that, for both O_2 and CO_2, the soot sample reactivity decreased when increasing the formation temperature of the soot sample. We attribute this to a graphitization process as the soot formation temperature increases. For both oxidation and gasification, the reactivity decreased by a factor of about 27 when increasing the soot formation temperature from 1275 to 1475 K. However, with regard to the influence of the gas environment during the formation of the soot, appreciable differences in the reactivity have been found only for the soot formed at 1475 K in N_2 and 78.5% CO_2 when oxidized with 5% O_2. For this soot, the reactivity was observed to increase by a factor of about 2.6 compared to soot formed in N_2 at the same temperature. We attribute the increased reactivity to a higher micropore surface
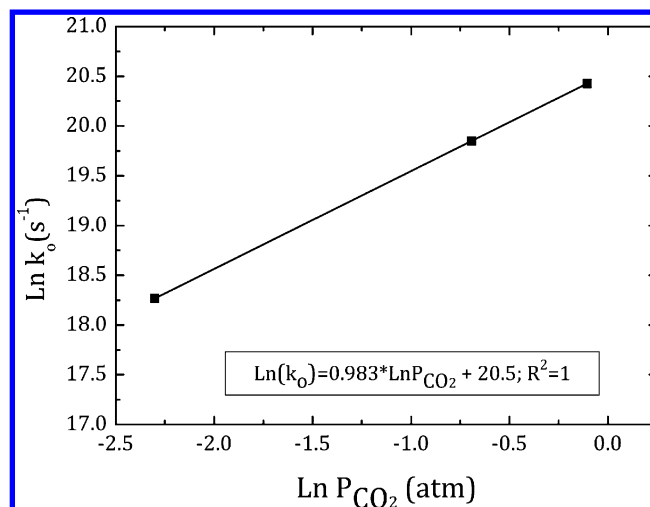
Figure 10. Determination of the reaction order with respect to CO_2 according to eq 3 in the gasification of soot sample 12 in Table 1 with 10, 50, and 90% CO_2.

area, facilitated by the gasification reaction at high temperatures. For all soot samples analyzed, oxidation by O_2 was initiated at much lower temperatures (about 450 K) than gasification by CO_2.

Intrinsic kinetics in terms of Arrhenius parameters by applying the volumetric reaction model (VRM) for oxidation and gasification of soot samples has been obtained from the reactivity profiles. The activation energy for oxidation of the different soot samples was in the range of 152−235 kJ/mol, while for gasification, it was 279−347 kJ/mol. A common activation energy of 182 kJ/mol for oxidation and 326 kJ/mol for gasification fitted the data fairly well. The reaction order with respect to CO_2 was found to be 0.98.

■ AUTHOR INFORMATION

Corresponding Author
*E-mail: uxue@unizar.es.

Notes
The authors declare no competing financial interest.

■ ACKNOWLEDGMENTS

■ REFERENCES

(1) Stanmore, B. R.; Brilhac, J. F.; Gilot, P. *Carbon* **2001**, *39*, 2247−2268.
(2) Ruiz, M. P.; Callejas, A.; Millera, A.; Alzueta, M. U.; Bilbao, R. *Int. J. Chem. React. Eng.* **2007**, *5*, A50.
(3) Mendiara, T.; Alzueta, M. U.; Millera, A.; Bilbao, R. *Energy Fuels* **2008**, *22*, 284−290.
(4) Buhre, B. J. P.; Elliott, L. K.; Sheng, C. D.; Gupta, R. P.; Wall, T. F. *Prog. Energy Combust. Sci.* **2005**, *31*, 283−307.
(5) Toftegaard, M. B.; Brix, J.; Jensen, P. A.; Glarborg, P.; Jensen, A. D. *Prog. Energy Combust. Sci.* **2010**, *36*, 581−625.

(6) Hurt, R. H.; Sarofim, A. F.; Longwell, J. P. *Combust. Flame* **1993**, *95*, 430−432.

(7) Ruiz, M. P.; Guzman de Villoria, R.; Millera, A.; Alzueta, M. U.; Bilbao, R. *Chem. Eng. J.* **2007**, *127*, 1−9.

(8) Borrego, A. G.; Álvarez, D. *Energy Fuels* **2007**, *21*, 3171−3179.

(9) Várhegyi, G.; Szabó, P.; Jakab, E.; Till, F. *Energy Fuels* **1996**, *10*, 1208−1214.

(10) Duan, L.; Zhao, C.; Zhou, W.; Qu, C.; Chen, X. *Energy Fuels* **2009**, *23*, 3826−3830.

(11) Li, Q.; Zhao, C.; Chen, X.; Wu, W.; Li, Y. *J. Anal. Appl. Pyrolysis* **2009**, *85*, 521−528.

(12) Rathnam, R. K.; Elliott, L. K.; Wall, T. F.; Liu, Y.; Moghtaderi, B. *Fuel Process. Technol.* **2009**, *90*, 797−802.

(13) Ruiz, M. P.; Guzman de Villoria, R.; Millera, A.; Alzueta, M. U.; Bilbao, R. *Ind. Eng. Chem. Res.* **2007**, *46*, 7550−7560.

(14) Esarte, C.; Millera, A.; Bilbao, R.; Alzueta, M. U. *Fuel Process. Technol.* **2009**, *90*, 496−503.

(15) Zolin, A.; Jensen, A. D.; Jensen, P. A.; Dam-Johansen, K. *Fuel* **2002**, *81*, 1065−1075.

(16) Rodríguez-Fernández, J.; Oliva, F.; Vázquez, R. A. *Energy Fuels* **2011**, *25*, 2039−2048.

(17) Zolin, A.; Jensen, A.; Pedersen, L. S.; Dam-Johansen, K.; Tørslev, P. *Energy Fuels* **1998**, *12*, 268−276.

(18) Russell, N. V.; Beeley, T. J.; Man, C.-K.; Gibbins, J. R.; Williamson, J. *Fuel Process. Technol.* **1998**, *57*, 113−130.

(19) Zhang, H.; Pu, W.-X.; Ha, S.; Li, Y.; Sun, M. *Fuel* **2009**, *88*, 2303−2310.

(20) Shim, H.-S.; Hurt, R. H. *Energy Fuels* **2000**, *14*, 340−348.

(21) Rockne, K. J.; Taghon, G. L.; Kosson, D. S. *Chemosphere* **2000**, *41*, 1125−1135.

(22) Guerrero, M.; Ruiz, M. P.; Alzueta, M. U.; Bilbao, R.; Millera, A. *J. Anal. Appl. Pyrolysis* **2005**, *74* (2005), 307−314.

(23) Dutta, S.; Wen, C. Y.; Belt, R. J. *Ind. Eng. Chem. Process Des. Dev.* **1977**, *16* (1), 20−30.

(24) Gilot, P.; Bonnefoy, F.; Marcuccilli, F.; Prado, G. *Combust. Flame* **1993**, *95*, 87−100.

(25) Mendiara, T.; Alzueta, M. U.; Millera, A.; Bilbao, R. *Energy Fuels* **2007**, *21*, 3208−3215.

(26) Liu, H.; Luo, C.; Toyota, M.; Uemiya, S.; Kojima, T. *Fuel Process. Technol.* **2006**, *87*, 769−774.